

University of New Hampshire

University of New Hampshire Scholars' Repository

Physics Scholarship

Physics

5-16-2015

Disappearance of plasmaspheric hiss following interplanetary shock

Zhenpeng Su

University of Science and Technology of China

Hui Zhu

University of Science and Technology of China

Fuliang Xiao

Changsha University of Science and Technology

Yuming Wang

University of Science and Technology of China

Chao Shen

Chinese Academy of Sciences, Beijing

See next page for additional authors

Follow this and additional works at: https://scholars.unh.edu/physics_facpub



Part of the [Astrophysics and Astronomy Commons](#)

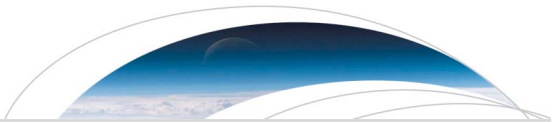
Recommended Citation

Z. Su, H. Zhu, F. Xiao, H. Zheng, Y. Wang, C. Shen, M. Zhang, S. Wang, C. A. Kletzing, W. S. Kurth, G. B. Hospodarsky, H. E. Spence, G. D. Reeves, H. O. Funsten, J. B. Blake, D. N. Baker, and J. R. Wygant, 'Disappearance of plasmaspheric hiss following interplanetary shock', *Geophysical Research Letters*, vol. 42, no. 9, pp. 3129–3140, May 2015.

This Article is brought to you for free and open access by the Physics at University of New Hampshire Scholars' Repository. It has been accepted for inclusion in Physics Scholarship by an authorized administrator of University of New Hampshire Scholars' Repository. For more information, please contact Scholarly.Communication@unh.edu.

Authors

Zhenpeng Su, Hui Zhu, Fuliang Xiao, Yuming Wang, Chao Shen, Min Zhang, Shui Wang, C A. Kletzing, W. S. Kurth, G. B. Hospodarsky, Harlan E. Spence, Geoffrey Reeves, H. O. Funsten, J. B. Blake, D. N. Baker, and J. R. Wygant



Geophysical Research Letters

RESEARCH LETTER

10.1002/2015GL063906

Key Points:

- First report on shock-induced disappearance of plasmaspheric hiss
- Interruption of chorus access into plasmasphere by enhanced Landau damping
- Removal of source electrons for chorus by the shrinking magnetopause

Correspondence to:

Z. Su,
szpe@mail.ustc.edu.cn

Citation:

Su, Z., et al. (2015), Disappearance of plasmaspheric hiss following interplanetary shock, *Geophys. Res. Lett.*, 42, 3129–3140,
doi:10.1002/2015GL063906.

Received 18 MAR 2015

Accepted 20 MAR 2015

Accepted article online 25 MAR 2015

Published online 12 May 2015

Disappearance of plasmaspheric hiss following interplanetary shock

Zhenpeng Su^{1,2,3}, Hui Zhu^{1,2,3,4}, Fuliang Xiao⁵, Huinan Zheng^{1,2,3}, Yuming Wang^{1,3}, Chao Shen⁶, Min Zhang¹, Shui Wang¹, C. A. Kletzing⁷, W. S. Kurth⁷, G. B. Hospodarsky⁷, H. E. Spence⁸, G. D. Reeves⁹, H. O. Funsten¹⁰, J. B. Blake¹¹, D. N. Baker¹², and J. R. Wygant¹³

¹CAS Key Laboratory of Geospace Environment, Department of Geophysics and Planetary Sciences, University of Science and Technology of China, Hefei, China, ²State Key Laboratory of Space Weather, Chinese Academy of Sciences, Beijing, China, ³Collaborative Innovation Center of Astronautical Science and Technology, Hefei, China, ⁴Mengcheng National Geophysical Observatory, School of Earth and Space Sciences, University of Science and Technology of China, Hefei, China, ⁵School of Physics and Electronic Sciences, Changsha University of Science and Technology, Changsha, China, ⁶State Key Laboratory of Space Weather, Center for Space Science and Applied Research, Chinese Academy of Sciences, Beijing, China, ⁷Department of Physics and Astronomy, University of Iowa, Iowa City, Iowa, USA, ⁸Institute for the Study of Earth, Oceans, and Space, University of New Hampshire, Durham, New Hampshire, USA, ⁹Space Science and Applications Group, Los Alamos National Laboratory, Los Alamos, New Mexico, USA, ¹⁰ISR Division, Los Alamos National Laboratory, Los Alamos, New Mexico, USA, ¹¹The Aerospace Corporation, Los Angeles, California, USA, ¹²Laboratory for Atmospheric and Space Physics, University of Colorado Boulder, Boulder, Colorado, USA, ¹³School of Physics and Astronomy, University of Minnesota, Twin Cities, Minnesota, USA

Abstract Plasmaspheric hiss is one of the important plasma waves controlling radiation belt dynamics. Its spatiotemporal distribution and generation mechanism are presently the object of active research. We here give the first report on the shock-induced disappearance of plasmaspheric hiss observed by the Van Allen Probes on 8 October 2013. This special event exhibits the dramatic variability of plasmaspheric hiss and provides a good opportunity to test its generation mechanisms. The origination of plasmaspheric hiss from plasmatrough chorus is suggested to be an appropriate prerequisite to explain this event. The shock increased the suprathermal electron fluxes, and then the enhanced Landau damping promptly prevented chorus waves from entering the plasmasphere. Subsequently, the shrinking magnetopause removed the source electrons for chorus, contributing significantly to the several-hours-long disappearance of plasmaspheric hiss.

1. Introduction

Plasmaspheric hiss is a broadband whistler mode emission in the terrestrial plasmasphere and plasmaspheric plumes [Russell *et al.*, 1969; Thorne *et al.*, 1973; Summers *et al.*, 2008]. It was widely considered to be structureless and incoherent, but its fine structures have been reported recently [Summers *et al.*, 2014]. Hiss waves typically occur in the frequency range from ~ 0.1 kHz to several kilohertz [Hayakawa and Sazhin, 1992] and even extend to the lower frequency 20 Hz [Li *et al.*, 2013]. The generation mechanism for plasmaspheric hiss is still under debate. Candidate mechanisms include the excitation by electron cyclotron instability in the outer plasmasphere [Thorne *et al.*, 1979; Chen *et al.*, 2014; Summers *et al.*, 2014], and the origination from lightning whistlers [e.g., Sonwalkar and Inan, 1989; Green *et al.*, 2005] or whistler mode chorus waves outside of the plasmasphere [Bortnik *et al.*, 2008, 2009].

Through cyclotron resonance, hiss waves can cause the pitch angle scattering of radiation belt electrons over a wide energy range from ~ 0.1 MeV to several MeV [Horne and Thorne, 1998; Summers *et al.*, 1998]. Such physical process contributes to the formation of the slot region separating the inner and outer radiation belts during quiet times [e.g., Lyons and Thorne, 1973; Abel and Thorne, 1998; Albert, 1994; Meredith *et al.*, 2007] and the precipitation loss of outer radiation belt electrons during storm times [e.g., Li *et al.*, 2007; Shprits *et al.*, 2009; Su *et al.*, 2011a; Mourenas and Ripoll, 2012; Thorne *et al.*, 2013; Ni *et al.*, 2014]. Hence, the information on the global spatiotemporal distribution of hiss is required to understand and/or predict the evolution of the electron radiation belt [Shprits *et al.*, 2009; Subbotin *et al.*, 2010; Su *et al.*, 2010, 2011b; Tu *et al.*, 2013; Glauert *et al.*, 2014]. Based on the CRRES observations, Meredith *et al.*, [2004, 2007] showed the statistical dependence of

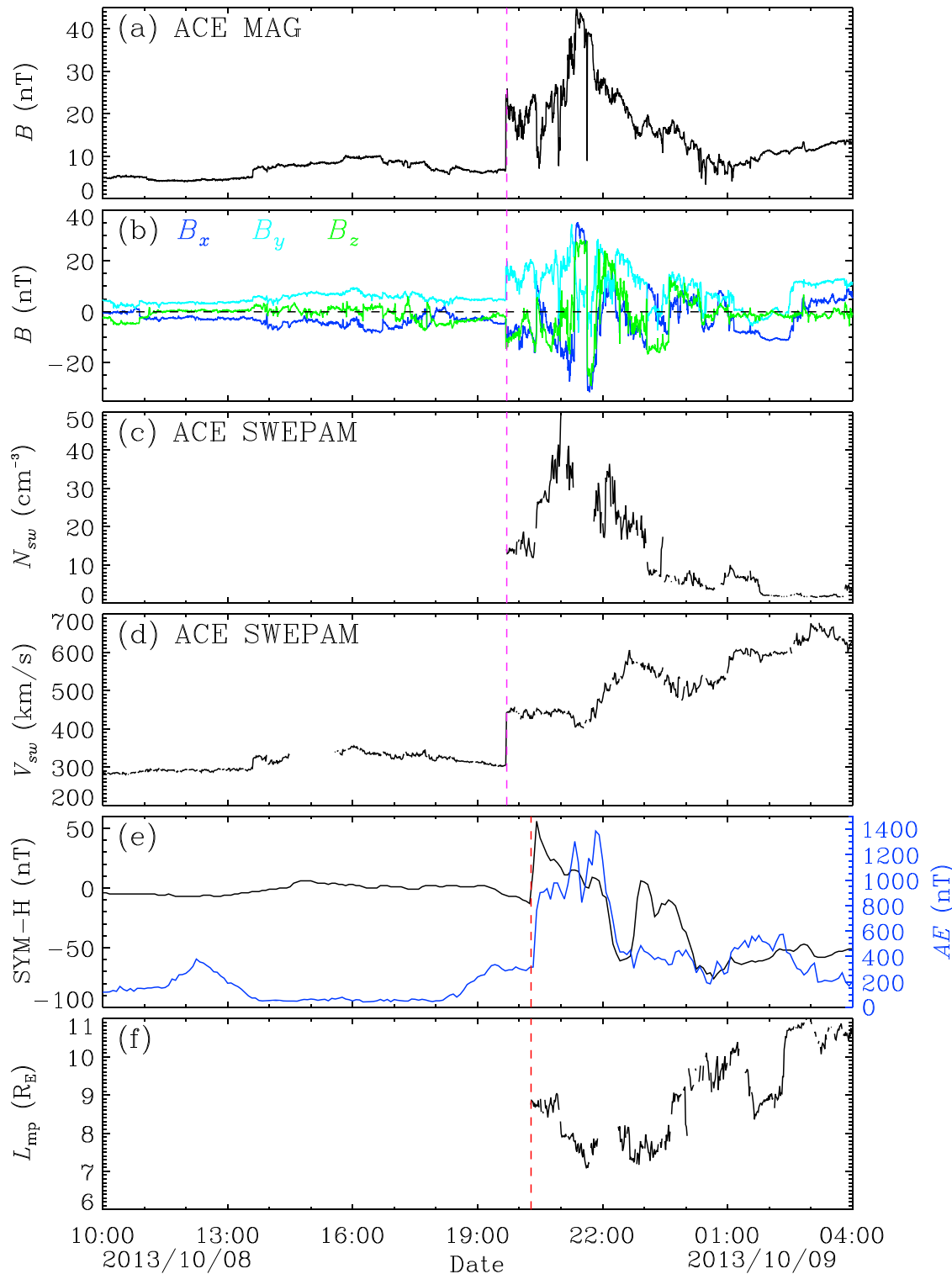


Figure 1. Interplanetary and magnetospheric parameters: (a) solar wind magnetic field magnitude B ; (b) three components (B_x , B_y , and B_z) of solar wind magnetic field in the GSM coordinate system; (c) solar wind proton number density N_{sw} ; (d) solar wind bulk speed V_{sw} ; (e) geomagnetic activity indices SYM-H and AE ; (f) magnetopause nose location L_{mp} .

hiss waves on substorm activity. Based on the THEMIS observations, *Golden et al.* [2012] gave a statistical hiss distribution model driven by solar wind parameters and geomagnetic activity indices. Based on the Cluster observations, *Agapitov et al.* [2013] presented the statistical characteristics of hiss wave normal angles. Based on the Polar observations, *Tsurutani et al.* [2015] emphasized the influence of solar wind ram pressure on hiss waves. However, it remains to be determined to what extent these statistical models can reproduce the realistic variability of hiss waves.

In this letter, we report a plasmaspheric hiss event observed by the Van Allen Radiation Belt Storm Probes (RBSP) [Mauk et al., 2013] during 8–9 October 2013. An interplanetary shock triggered a strong substorm (with maximum $AE \approx 1400$ nT) but simultaneously quenched the plasmaspheric hiss for about 5 h, contrary to the statistical picture that strong substorm [Meredith et al., 2004] or solar wind with high ram pressure [Tsurutani et al., 2015] enhance hiss activity. Note that *Thorne et al.* [1974] had reported two substorm events with the reduction of duskside hiss. To our best knowledge, this is the first report on the shock-induced disappearance of plasmaspheric hiss. This special event exhibits the significant and complex variability of plasmaspheric hiss and provides a good opportunity to test the generation mechanisms for plasmaspheric hiss.

2. Event Overview

Figure 1 plots the interplanetary and magnetospheric parameters from 10:00 UT on 8 October 2013 to 04:00 UT on 9 October 2013. The solar wind magnetic field \mathbf{B} , ion number density N_{sw} and bulk speed V_{sw} were observed by the Magnetic Fields Experiment [Smith et al., 1998] and the Solar Wind Electron, Proton, and Alpha Monitor [McComas et al., 1998] on board the Advanced Composition Explorer [Stone et al., 1998]. The time-shifted interplanetary parameters can be used to determine the location of the magnetopause [Shue et al., 1998]. The geomagnetic indices $SYM-H$ and AE were provided by the World Data Center for Geomagnetism, Kyoto. The interplanetary shock driven by a coronal mass ejection can be clearly identified at 19:42 UT on 8 October 2013. After about 35 min, the shock compressed the magnetosphere (with the magnetopause nose shrinking to $L_{mp} \sim 8.5$) and caused the geomagnetic storm sudden commencement (abrupt increase of $SYM-H$ index from -10 nT to 50 nT). Slightly later, the shock further triggered a strong substorm with the maximum $AE \approx 1400$ nT.

Figure 2 shows the waves observed by the Electric and Magnetic Field Instrument Suite and Integrated Science instrument suite (EMFISIS) [Kletzing et al., 2013] on board the twin RBSP satellites. The time range from 10:00 UT on 8 October 2013 to 04:00 UT on 9 October 2013 covered approximately two orbital periods of the RBSP satellites. At the shock arrival time (corresponding to the peak of $SYM-H$), the RBSP-A satellite was in the slot region ($L \approx 3.3$) and the RBSP-B satellite was approximately at the center of outer radiation belt ($L \approx 5.3$). The upper hybrid resonance bands (bright lines) were clearly visible in the electric power spectral densities (Figures 2a and 2c) of the High-Frequency Receiver (HFR). These upper hybrid frequencies (positively correlated with the background electron density [Kurth et al., 2014]) were above 60 kHz most of the time, indicating the locations of RBSP satellites in the plasmasphere. In the HFR channel, the shock-induced disturbances were quite evident for RBSP-B but invisible for RBSP-A. The plasmaspheric hiss waves with frequencies from 50 Hz to 1 kHz (Figures 2b and 2d) were detected by the Waveform Receiver (WFR). In the first orbital period, both RBSP satellites almost continuously received hiss waves. Around 13:00 UT on 8 October 2013, there was an intensification in the hiss spectrums of both RBSP satellites, probably caused by a weak substorm (Figure 1e). Around 17:00 UT on 8 October 2013, the hiss intensity observed by RBSP-A was modulated by the background electron density [Chen et al., 2012d]. In the second orbital period, the hiss observed by both RBSP satellites abruptly ceased at the peak of the $SYM-H$ index. After about 5 h, the hiss waves recovered with much stronger intensities (Figure 2d).

Figures 3 and 4 present the observations of background electron distributions and electromagnetic fields by the twin RBSP satellites. The omnidirectional/differential electron fluxes were collected by the Helium Oxygen Proton Electron (HOPE) Mass Spectrometer [Funsten et al., 2013], Magnetic Electron Ion Spectrometer (MagEIS) [Blake et al., 2013], and Relativistic Electron-Proton Telescope (REPT) [Baker et al., 2013] of the Energetic Particle, Composition, and Thermal Plasma (ECT) suite [Spence et al., 2013]. The magnetic field and electric field were provided by the EMFISIS Magnetometer and Electric Fields and Waves (EFW) instruments [Wygant et al., 2013]. For the electron fluxes over a wide energy range, the RBSP-A observations responded weakly to the shock arrival, but the RBSP-B observations exhibited a sudden enhancement up to 2 orders of magnitude with the shock arrival. When the RBSP-A satellite went into the outer region ($L > 3.6$), it observed the drift echoes of

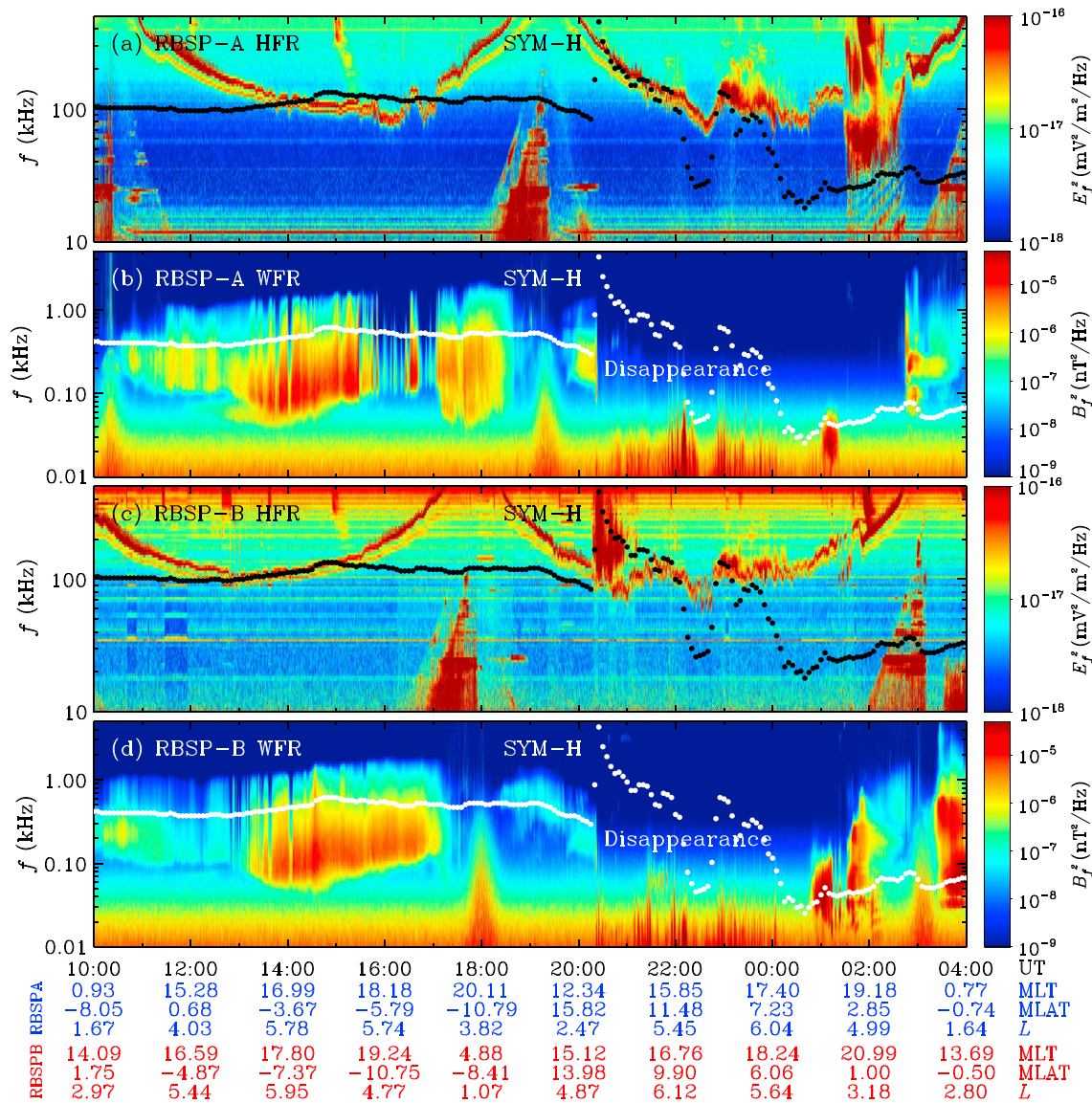


Figure 2. (a–d) Electric/magnetic field spectral density in the HFR/WFR channels observed by the twin RBSP satellites. Note that the superposed solid dots represent the SYM-H index.

relativistic electrons (Figure 3d). Both spacecraft detected an increase in the magnetic field strength after the shock hit (most easily observed in Figure 4e due to the lower preshock field). The shock-induced variation in electric fields detected by both RBSP satellites had comparable peak amplitudes (10 mV/m) but different fluctuating periods (~ 3 min for RBSP-A and ~ 6 min for RBSP-B).

3. Discussion

There are generally three candidate generation mechanisms for plasmaspheric hiss (see section 1). Considering the poor connection between lightning and shock, we exclude the origination from lightning whistlers [Sonwalkar and Inan, 1989; Green et al., 2005]. If plasmaspheric hiss originates from plammatrough chorus [e.g., Bortnik et al., 2008, 2009; Chen et al., 2012c], the following four stages would be involved: (1) excitation of chorus outside the plasmasphere, (2) propagation and Landau damping or cyclotron amplification of chorus, (3) refraction of chorus into the plasmasphere, and (4) amplification of hiss within the plasmasphere. In fact, the isolated occurrence of the fourth stage corresponds to the other generation mechanism, excitation by electron cyclotron instability [e.g., Thorne et al., 1979; Chen et al., 2014; Summers et al., 2014]. Obviously, the first

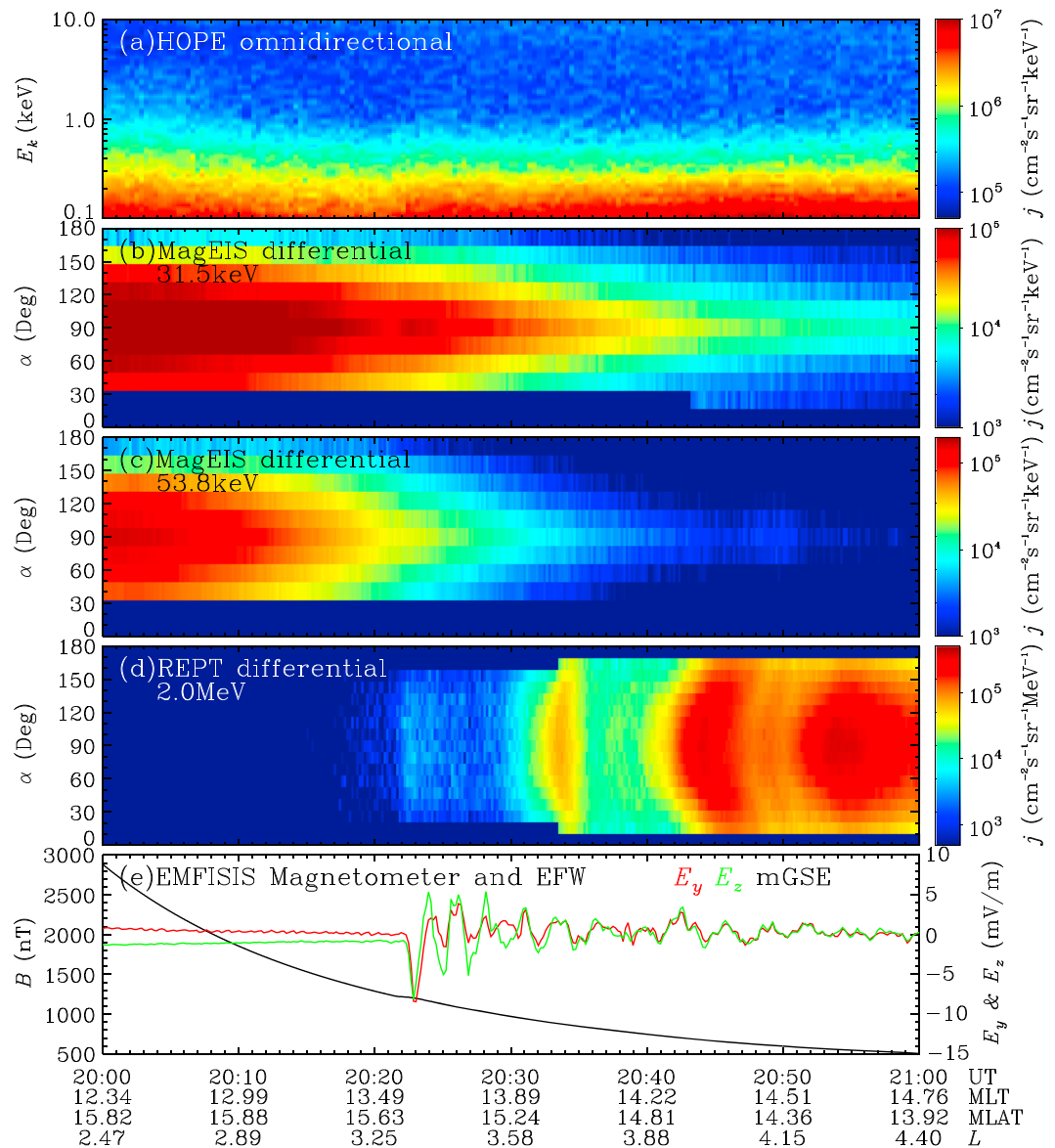


Figure 3. RBSP-A observations on the (a–d) omnidirectional/differential electron fluxes and (e) electromagnetic fields around the shock arrival time.

three stages depend significantly on the electron distributions in the plasmatrough, unavailable due to the limited orbital coverage of the RBSP satellites. The fourth stage is controlled by the plasmaspheric electron distribution, available at the RBSP orbital regions. Here we first infer the global response of inner magnetospheric plasma to the shock and then discuss the potential effects of the shock on all four stages.

3.1. Inner Magnetospheric Plasma Response

The shock caused the prompt acceleration of electrons over a wide range of energies and pitch angles (Figures 3 and 4). The relativistic (MeV) electron flux enhancement occurred in the region $L \gtrsim 3.6$, while the suprathermal (keV to tens of keV) electron flux enhancement primarily emerged in the outer region $L \gtrsim 5$. The possible energization mechanisms include the following: (1) betatron acceleration (conserving the first adiabatic invariant), (2) Fermi acceleration (conserving the second adiabatic invariant), and (3) parallel electric field acceleration. For the high-energy electrons, the betatron/Fermi acceleration might be dominant [Li *et al.*, 1993; Hudson *et al.*, 1997; Foster *et al.*, 2015]. For the low-energy electrons, the Fermi acceleration was not applicable due to the long bounce period [Ukhorskiy and Sitnov, 2013], and the betatron acceleration and the parallel electric field acceleration might be dominant [e.g., Tsurutani *et al.*, 2001; Peng *et al.*, 2011].

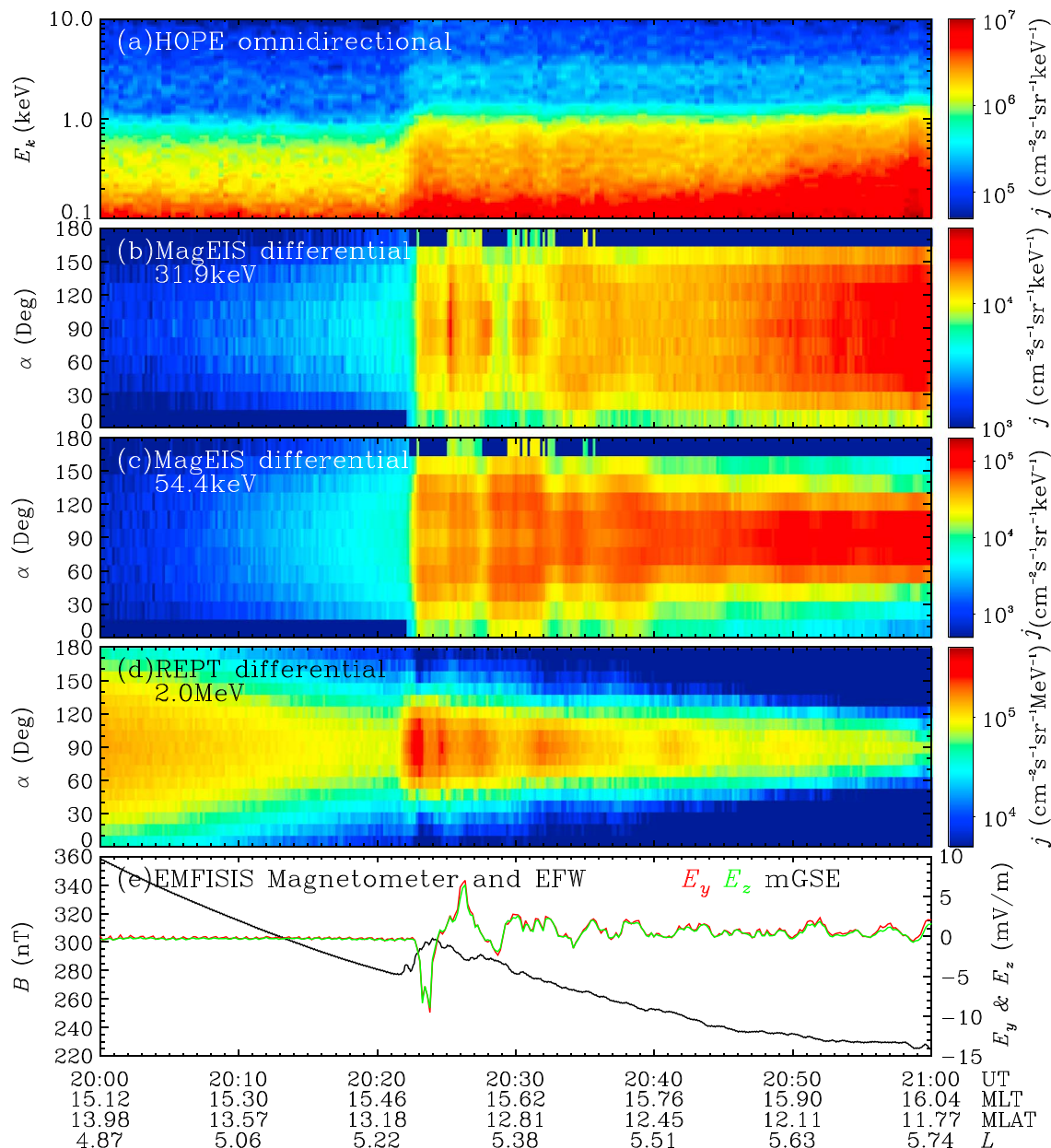


Figure 4. RBSP-B observations on the (a–d) omnidirectional/differential electron fluxes and (e) electromagnetic fields around the shock arrival time.

A detailed and accurate analysis of the electron energization process is beyond the scope of this letter and is left for future investigation.

In addition, the shock and the subsequent coronal mass ejection could highly compress the magnetosphere and remove the outer magnetospheric plasma through the “magnetopause shadowing” process [e.g., Turner *et al.*, 2012]. The shock-induced compression of the plasmasphere could also occur, as shown in previous simulations [e.g., Samsonov *et al.*, 2007] and observations [e.g., Zhang *et al.*, 2012]. During the geomagnetic storm driven by the shock and the subsequent coronal mass ejection, the plasmaspheric plume might gradually form due to the enhanced convection electric field [e.g., Goldstein *et al.*, 2005].

3.2. Excitation of Chorus Outside the Plasmasphere

Generally speaking, the chorus waves are excited through the cyclotron resonance with anisotropic suprathermal electrons [e.g., Kennel and Petschek, 1966; Nunn *et al.*, 1997; Omura *et al.*, 2008; Li *et al.*, 2009]. As discussed in section 3.1, we expect a prompt increase of suprathermal electron fluxes after the shock, which could

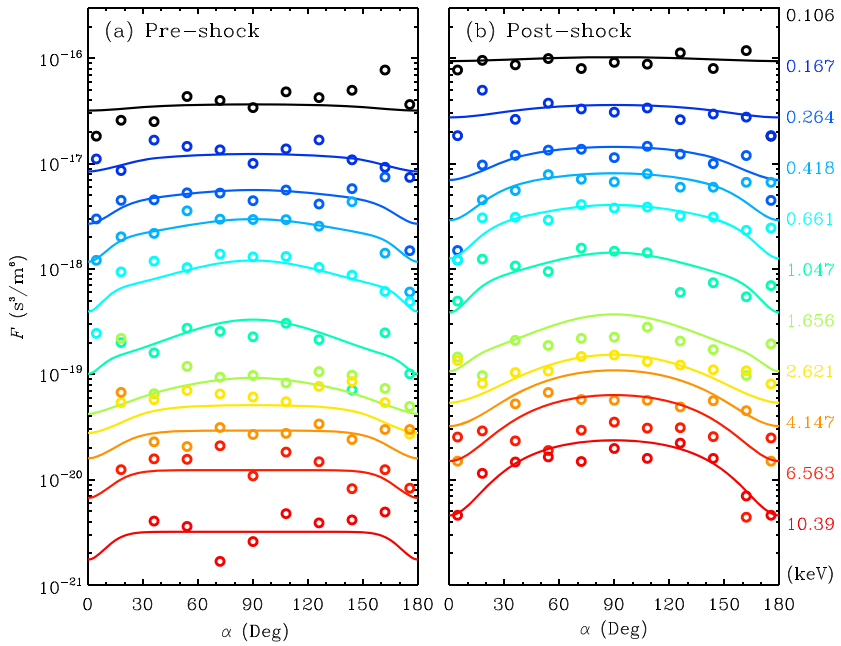


Figure 5. Suprathermal electron PSDs (a) before and (b) after shock at $L = 8.0$ with circles for the hypothetical observations and lines for the simulations. Note that the suprathermal electron PSDs in the plasmatrough ($L = 8.0$) have been assumed to be the tenfold of those observed by RBSP-B in the plasmasphere ($L = 5.3$).

favor the excitation of chorus waves. Without the subsequent chorus damping during propagation (see section 3.3), such prompt energization process would intensify (rather than reduce) the plasmaspheric hiss. During 21:00–24:00 UT on 8 October 2013, the magnetopause nose shrank to about $L_{mp} = 7–8$ (see Figure 1f), quite close to the preshock plasmapause $L \gtrsim 6.2$ (Figure 2). The drastic removal of source electrons for chorus by the magnetopause shadowing could contribute largely to the several-hours-long disappearance of plasmaspheric hiss waves.

3.3. Propagation and Landau Damping or Cyclotron Amplification of Chorus

The chorus waves experience Landau damping/cyclotron amplification by the suprathermal electrons in the course of propagation toward higher latitudes [e.g., *Bortnik et al.*, 2011; *Chen et al.*, 2012a]. The intuitive idea is that the enhanced Landau damping would interrupt the propagation of chorus. We attempt here to estimate the shock-induced variation in the Landau damping rate.

Considering that the plasmasphere had extended to at least $L = 6.2$ (Figure 2), we specifically calculate the Landau damping rates at a selected plasmatrough location $L = 8$. Based on the statistical results of *Li et al.* [2010], we assume that the suprathermal electron fluxes at $L = 8$ equaled tenfold of those observed by RBSP-B in the outer plasmasphere at $L = 5.3$. Figure 5 shows the “hypothetically observed” (circles) and modeled (lines) suprathermal electron phase space density (PSD) before and after the shock arrival. The modeled PSD F contains $N = 4$ components

$$F(v_{\perp}, v_{\parallel}) = \sum_{i=1}^N F_i, \quad (1)$$

$$F_i = \frac{n_i}{(\sqrt{\pi} V_{th,i})^3} \exp \left[- \left(\frac{v_{\parallel}}{V_{th,i}} - V_{dr,i} \right)^2 \right] \times \left\{ \frac{\Delta_i}{\alpha_{1,i}} \exp \left(- \frac{v_{\perp}^2}{\alpha_{1,i} V_{th,i}^2} \right) + \frac{1 - \Delta_i}{\alpha_{1,i} - \alpha_{2,i}} \right. \\ \left. \times \left[\exp \left(- \frac{v_{\perp}^2}{\alpha_{1,i} V_{th,i}^2} \right) - \exp \left(- \frac{v_{\perp}^2}{\alpha_{2,i} V_{th,i}^2} \right) \right] \right\}. \quad (2)$$

For the i th plasma component, n_i is the density, $V_{th,i} = \sqrt{2T_i/m_e}$ and $V_{dr,i}$ are the field-aligned thermal velocity and the normalized drift velocity, $\alpha_{1,i}$ and $\alpha_{2,i}$ characterize the temperature anisotropy and the size of loss cone, and Δ_i controls the depth of loss cone. The total electron number density is taken to be constant

Table 1. Fitting Parameters for Electron PSDs Before and After the Shock

Component	$n_i(\text{m}^{-3})$	$T_i(\text{keV})$	Δ_i	$\alpha_{1,i}$	$\alpha_{2,i}$	V_{dr_i}
<i>Pre</i>						
1	2.2900×10^6	0.0028	1.0000	1.0000	0.5000	0
2	1.3000×10^5	0.0348	1.0000	1.0000	0.5000	0
3	6.0000×10^4	0.2054	0.6000	1.2491	0.1249	0
4	2.0000×10^4	2.7321	0.6000	1.0000	0.2000	0
<i>Post</i>						
1	1.9550×10^6	0.0028	1.0000	1.0000	0.5000	0
2	3.2000×10^5	0.0432	1.0000	1.0000	0.5000	0
3	1.6000×10^5	0.2843	0.5000	1.2100	0.2420	0
4	6.5000×10^4	3.0960	0.4000	1.0615	0.6369	0

$N_e = 2.5 \times 10^6 \text{ m}^{-3}$ [Sheeley et al., 2001]. Adopting those parameters listed in Table 1 leads to reasonable agreements between the modeled and hypothetically observed distributions. Clearly, the suprathermal electron PSDs increased by a factor of 2–6 with the larger anisotropy after the shock.

These energy and pitch angle-dependent PSDs can be used to analyze the amplification/damping of plasma waves [e.g., Kennel and Engelmann, 1966; Shklyar, 2011; Su et al., 2014]. Figure 6 presents the calculated damping rates using the Waves in Homogeneous Anisotropic Magnetized Plasma (WHAMP) code [Ronnmark, 1982]. The background magnetic field is specified as $B = 61 \text{ nT}$ (i.e., the equatorial magnetic strength at $L = 8$ in the typical dipole field), and the wave frequency is selected as $f = 200 \text{ Hz}$ (i.e., the peak frequency of hiss spectrum in Figure 2). It is found that the damping rate increased by a factor of ~ 3 –5 for waves with normal angles $\psi > 20^\circ$. As illustrated in the previous ray-tracing simulations [Bortnik et al., 2011; Chen et al., 2012a], the chorus rays that can access the plasmasphere usually have wave normal angles $\psi \approx 40^\circ$ – 70° . The intensities of these chorus rays with $\psi \approx 40^\circ$ – 70° could be reduced to much less than 1% within 1 s after the shock. Such enhanced Landau damping might be responsible for quenching plasmaspheric hiss [Bortnik et al., 2007].

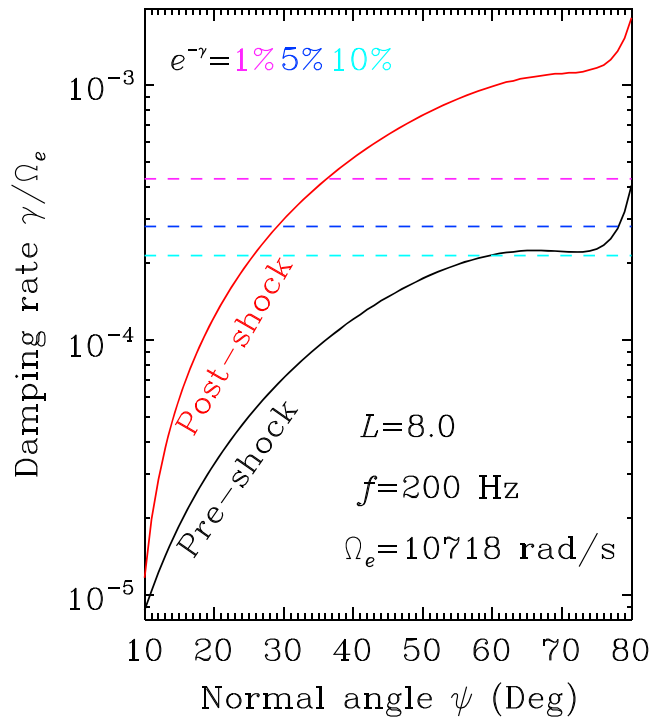


Figure 6. Normal-angle ψ -dependent damping rate γ for the $f = 200 \text{ Hz}$ chorus waves at $L = 8.0$ during the preshock/postshock times. Note that the dashed horizontal lines denote the damping rates satisfying the relations $e^{-\gamma} = 1\%$ (magenta), 5% (blue), and 10% (cyan).

It should be mentioned that the WHAMP code fully includes the Landau damping and cyclotron amplification processes. For the present simulations, the preshock PSD with the weak anisotropy did not allow the effective amplification of waves at any normal angles, while the postshock PSD with the moderate anisotropy could amplify waves at the normal angles $\psi < 10^\circ$ (not shown).

3.4. Refraction of Chorus Into the Plasmasphere

The refraction is considered to be controlled by the cold electron distribution. *Chen et al.* [2012b] have demonstrated that the location or width of the plasmapause do not affect the peak hiss intensity significantly. Hence, the potential change of plasmapause by the shock was difficult to explain the prompt disappearance of plasmaspheric hiss. However, *Chen et al.* [2009] have suggested that the location and width of the plasmaspheric plume control the access of chorus waves into the duskside plasmasphere. Within several hours after the shock, the contribution of the evolving plasmaspheric plume to the hiss disappearance may need further investigation.

3.5. Amplification of Hiss Within the Plasmasphere

The amplification rate of hiss waves depends on the suprathermal/energetic electron distribution [*Chen et al.*, 2012c]. As observed by the RBSP satellites (Figures 3a and 4a), the suprathermal/energetic electron fluxes exhibited significant enhancement in the outer plasmasphere, promoting the amplification of injected chorus [*Chen et al.*, 2012c] or thermal noise [*Thorne et al.*, 1979]. Hence, the shock-induced change in this stage was unable to quench plasmaspheric hiss.

4. Conclusions

Plasmaspheric hiss plays an important role in radiation belt dynamics during both quiet and storm times. Its global spatiotemporal distributions have been statistically investigated [*Meredith et al.*, 2004, 2007; *Golden et al.*, 2012; *Agapitov et al.*, 2013; *Tsurutani et al.*, 2015]. In a statistical sense, strong substorms or solar wind with high ram pressure can intensify the plasmaspheric hiss waves. Here we report an interesting counterexample provided by the RBSP satellites. Following the interplanetary shock on 8 October 2013, a strong substorm (with maximum $AE \approx 1400$ nT) occurred, but simultaneously the plasmaspheric hiss waves disappeared for about 5 h. These observations clearly illustrate the significant and complex variability of plasmaspheric hiss waves.

The generation mechanism for plasmaspheric hiss is still under debate. The origination of plasmaspheric hiss from plasmatrough chorus is suggested to be an appropriate prerequisite to explain this special event. The interplanetary shock produced the prompt acceleration of electrons over a wide range of energies and pitch angles. Landau damping in the plasmatrough, controlled by the suprathermal (0.1–10 keV) electron fluxes, might have become too strong to allow the access of chorus into plasmasphere. As suggested in previous works [*Bortnik et al.*, 2008, 2009], the interruption of energy injection by chorus could cause the disappearance of plasmaspheric hiss. Moreover, the shock and the subsequent coronal mass ejection continuously compressed the magnetosphere and largely removed the source electrons for chorus through the magnetopause shadowing process, which could contribute significantly to the several-hours-long disappearance of plasmaspheric hiss. We reiterate that the current explanations are obtained based on the inferred variations in the plasmatrough and magnetopause. The RBSP satellites, as well as the THEMIS or the Cluster satellites, were not in the appropriate positions to measure the dayside plasmatrough/magnetopause properties during the time period of interest. Future global magnetospheric simulations are required to examine the proposed explanations.

The influence of the solar wind on the inner magnetosphere has long been investigated in the space physics community [e.g., *Baker et al.*, 1983, 1998; *Gonzalez et al.*, 1989; *Reeves et al.*, 1998; *Wang et al.*, 2010]. Interplanetary shocks have been reported to trigger the substorms [*Heppner*, 1955], storms [*Gonzalez et al.*, 1994], auroral brightening [*Zhou and Tsurutani*, 1999; *Meurant et al.*, 2004; *Su et al.*, 2011c], magnetospheric particle energization [e.g., *Blake et al.*, 1992; *Hudson et al.*, 1997; *Zong et al.*, 2009], and chorus intensification [*Fu et al.*, 2012]. The current observations exhibit a potentially new consequence of interplanetary shock on the inner magnetosphere, the disappearance of plasmaspheric hiss.

Acknowledgments

The interplanetary parameters and geomagnetic indices are obtained at the CDAWeb (http://cdaweb.gsfc.nasa.gov/cdaweb/istp_public/). The RBSP data are available at the websites (<http://emfisis.physics.uiowa.edu/Flight/>, http://www.rbsp-ect.lanl.gov/data_pub/ for ECT, and <http://www.space.umn.edu/rbspefw-data/> for EFW). We acknowledge K. Ronnmark for the using of WHAMP code. This work was supported by the National Natural Science Foundation of China grants 41274169, 41274174, 41422405, 41174125, 41131065, 41121003, 41074120, 41231066, and 41304134; the Chinese Academy of Sciences grant KZCX2-EW-QN510 and KZZD-EW-01-4; and the National Key Basic Research Special Foundation of China grant 2011CB811403. This work was also supported from JHU/APL contracts 921647, 967399, and 922613 under NASA Prime contract NAS5-01072.

The Editor thanks two anonymous reviewers for their assistance in evaluating this paper.

References

- Abel, B., and R. M. Thorne (1998), Electron scattering loss in Earth's inner magnetosphere: 1. Dominant physical processes, *J. Geophys. Res.*, **103**, 2385–2396, doi:10.1029/97JA02919.
- Agapitov, O., A. Artemyev, V. Krasnoselskikh, Y. V. Khotyaintsev, D. Mourenas, H. Breuillard, M. Balikhin, and G. Rolland (2013), Statistics of whistler mode waves in the outer radiation belt: Cluster STAFF-SA measurements, *J. Geophys. Res. Space Physics*, **118**, 3407–3420, doi:10.1002/jgra.50312.
- Albert, J. M. (1994), Quasi-linear pitch angle diffusion coefficients: Retaining high harmonics, *J. Geophys. Res.*, **99**, 23,741–23,745, doi:10.1029/94JA02345.
- Baker, D. N., R. D. Zwickl, S. J. Bame, E. W. Hones Jr., B. T. Tsurutani, E. J. Smith, and S. -I. Akasofu (1983), An ISEE 3 high time resolution study of interplanetary parameter correlations with magnetospheric activity, *J. Geophys. Res.*, **88**, 6230–6242, doi:10.1029/JA088iA08p06230.
- Baker, D. N., T. I. Pulkkinen, X. Li, S. G. Kanekal, J. B. Blake, R. S. Selesnick, M. G. Henderson, G. D. Reeves, H. E. Spence, and G. Rostoker (1998), Coronal mass ejections, magnetic clouds, and relativistic magnetospheric electron events: ISTP, *J. Geophys. Res.*, **103**, 17,279–17,291, doi:10.1029/97JA03329.
- Baker, D. N., et al. (2013), The Relativistic Electron-Proton Telescope (REPT) instrument on board the Radiation Belt Storm Probes (RBSP) spacecraft: Characterization of Earth's radiation belt high-energy particle populations, *Space Sci. Rev.*, **179**, 337–381, doi:10.1007/s11214-012-9950-9.
- Blake, J. B., W. A. Kolasinski, R. W. Fillius, and E. G. Mullen (1992), Injection of electrons and protons with energies of tens of MeV into L less than 3 on 24 March 1991, *Geophys. Res. Lett.*, **19**, 821–824, doi:10.1029/92GL00624.
- Blake, J. B., et al. (2013), The magnetic electron ion spectrometer (MagEIS) instruments aboard the radiation belt storm probes (RBSP) spacecraft, *Space Sci. Rev.*, **179**, 383–421, doi:10.1007/s11214-013-9991-8.
- Bortnik, J., R. M. Thorne, and N. P. Meredith (2007), Modeling the propagation characteristics of chorus using CRRES suprathermal electron fluxes, *J. Geophys. Res.*, **112**, A08204, doi:10.1029/2006JA012237.
- Bortnik, J., R. M. Thorne, and N. P. Meredith (2008), The unexpected origin of plasmaspheric hiss from discrete chorus emissions, *Nature*, **452**, 62–66, doi:10.1038/nature06741.
- Bortnik, J., W. Li, R. M. Thorne, V. Angelopoulos, C. Cully, J. Bonnell, O. Le Contel, and A. Roux (2009), An observation linking the origin of plasmaspheric hiss to discrete chorus emissions, *Science*, **324**, 775–778, doi:10.1126/science.1171273.
- Bortnik, J., L. Chen, W. Li, R. M. Thorne, and R. B. Horne (2011), Modeling the evolution of chorus waves into plasmaspheric hiss, *J. Geophys. Res.*, **116**, A08221, doi:10.1029/2011JA016499.
- Chen, L., J. Bortnik, R. M. Thorne, R. B. Horne, and V. K. Jordanova (2009), Three-dimensional ray tracing of VLF waves in a magnetospheric environment containing a plasmaspheric plume, *Geophys. Res. Lett.*, **36**, L22101, doi:10.1029/2009GL040451.
- Chen, L., J. Bortnik, W. Li, R. M. Thorne, and R. B. Horne (2012a), Modeling the properties of plasmaspheric hiss: 1. Dependence on chorus wave emission, *J. Geophys. Res.*, **117**, A05201, doi:10.1029/2011JA017201.
- Chen, L., J. Bortnik, W. Li, R. M. Thorne, and R. B. Horne (2012b), Modeling the properties of plasmaspheric hiss: 2. Dependence on the plasma density distribution, *J. Geophys. Res.*, **117**, A05202, doi:10.1029/2011JA017202.
- Chen, L., W. Li, J. Bortnik, and R. M. Thorne (2012c), Amplification of whistler-mode hiss inside the plasmasphere, *Geophys. Res. Lett.*, **39**, L08111, doi:10.1029/2012GL051488.
- Chen, L., R. M. Thorne, W. Li, J. Bortnik, D. Turner, and V. Angelopoulos (2012d), Modulation of plasmaspheric hiss intensity by thermal plasma density structure, *Geophys. Res. Lett.*, **39**, L14103, doi:10.1029/2012GL052308.
- Chen, L., et al. (2014), Generation of unusually low frequency plasmaspheric hiss, *Geophys. Res. Lett.*, **41**, 5702–5709, doi:10.1002/2014GL060628.
- Foster, J. C., J. R. Wygant, M. K. Hudson, A. J. Boyd, D. N. Baker, P. J. Erickson, and H. E. Spence (2015), Shock-induced prompt relativistic electron acceleration in the inner magnetosphere, *J. Geophys. Res. Space Physics*, **120**, 1661–1674, doi:10.1002/2014JA020642.
- Fu, H. S., J. B. Cao, F. S. Mozer, H. Y. Lu, and B. Yang (2012), Chorus intensification in response to interplanetary shock, *J. Geophys. Res.*, **117**, A01203, doi:10.1029/2011JA016913.
- Funsten, H. O., et al. (2013), Helium, Oxygen, Proton, and Electron (HOPE) mass spectrometer for the radiation belt storm probes mission, *Space Sci. Rev.*, **179**, 423–484, doi:10.1007/s11214-013-9968-7.
- Glauert, S. A., R. B. Horne, and N. P. Meredith (2014), Three-dimensional electron radiation belt simulations using the BAS radiation belt model with new diffusion models for chorus, plasmaspheric hiss, and lightning-generated whistlers, *J. Geophys. Res. Space Physics*, **119**, 268–289, doi:10.1002/2013JA019281.
- Golden, D. I., M. Spasovic, W. Li, and Y. Nishimura (2012), Statistical modeling of plasmaspheric hiss amplitude using solar wind measurements and geomagnetic indices, *Geophys. Res. Lett.*, **39**, L06103, doi:10.1029/2012GL051185.
- Goldstein, J., B. R. Sandel, W. T. Forrester, M. F. Thomsen, and M. R. Hairston (2005), Global plasmasphere evolution 22–23 April 2001, *J. Geophys. Res.*, **110**, A12218, doi:10.1029/2005JA011282.
- Gonzalez, W. D., A. L. C. Gonzalez, B. T. Tsurutani, E. J. Smith, and F. Tang (1989), Solar wind-magnetosphere coupling during intense magnetic storms (1978–1979), *J. Geophys. Res.*, **94**, 8835–8851, doi:10.1029/JA094iA07p08835.
- Gonzalez, W. D., J. A. Joselyn, Y. Kamide, H. W. Kroehl, G. Rostoker, B. T. Tsurutani, and V. M. Vasiliunas (1994), What is a geomagnetic storm?, *J. Geophys. Res.*, **99**, 5771–5792.
- Green, J. L., S. Boardsen, L. Garcia, W. W. L. Taylor, S. F. Fung, and B. W. Reinisch (2005), On the origin of whistler mode radiation in the plasmasphere, *J. Geophys. Res.*, **110**, A03201, doi:10.1029/2004JA010495.
- Hayakawa, M., and S. S. Sazhin (1992), Mid-latitude and plasmaspheric hiss—A review, *Planet. Space Sci.*, **40**, 1325–1338, doi:10.1016/0032-0633(92)90089-7.
- Heppner, J. P. (1955), Note on the occurrence of world-wide SSCs during the onset of negative bays at College, Alaska, *J. Geophys. Res.*, **60**, 29–32, doi:10.1029/JZ060i001p00029.
- Horne, R. B., and R. M. Thorne (1998), Potential waves for relativistic electron scattering and stochastic acceleration during magnetic storms, *Geophys. Res. Lett.*, **25**, 3011–3014, doi:10.1029/98GL01002.
- Hudson, M. K., S. R. Elkington, J. G. Lyon, V. A. Marchenko, I. Roth, M. Temerin, J. B. Blake, M. S. Gussenhoven, and J. R. Wygant (1997), Simulations of radiation belt formation during storm sudden commencements, *J. Geophys. Res.*, **102**, 14,087–14,102, doi:10.1029/97JA03995.
- Kennel, C. F., and F. Engelmann (1966), Velocity space diffusion from weak plasma turbulence in a magnetic field, *Phys. Fluids*, **9**, 2377–2388, doi:10.1063/1.1761629.
- Kennel, C. F., and H. E. Petschek (1966), Limit on stably trapped particle fluxes, *J. Geophys. Res.*, **71**, 1–28.
- Kletzing, C. A., et al. (2013), The Electric and Magnetic Field Instrument Suite and Integrated Science (EMFISIS) on RBSP, *Space Sci. Rev.*, **179**, 127–181, doi:10.1007/s11214-013-9993-6.

- Kurth, W. S., S. D. Pascuale, J. B. Faden, C. A. Kletzing, G. B. Hospodarsky, S. Thaller, and J. R. Wygant (2014), Electron densities inferred from plasma wave spectra obtained by the waves instrument on Van Allen Probes, *J. Geophys. Res. Space Physics*, **120**, 904–914, doi:10.1002/2014JA020857.
- Li, W., Y. Y. Shprits, and R. M. Thorne (2007), Dynamic evolution of energetic outer zone electrons due to wave-particle interactions during storms, *J. Geophys. Res.*, **112**, A10220, doi:10.1029/2007JA012368.
- Li, W., R. M. Thorne, V. Angelopoulos, J. W. Bonnell, J. P. McFadden, C. W. Carlson, O. LeContel, A. Roux, K. H. Glassmeier, and H. U. Auster (2009), Evaluation of whistler-mode chorus intensification on the nightside during an injection event observed on the THEMIS spacecraft, *J. Geophys. Res.*, **114**, A00C14, doi:10.1029/2008JA013554.
- Li, W., R. M. Thorne, J. Bortnik, Y. Nishimura, V. Angelopoulos, L. Chen, J. P. McFadden, and J. W. Bonnell (2010), Global distributions of suprathermal electrons observed on THEMIS and potential mechanisms for access into the plasmasphere, *J. Geophys. Res.*, **115**, A00J10, doi:10.1029/2010JA015687.
- Li, W., et al. (2013), An unusual enhancement of low-frequency plasmaspheric hiss in the outer plasmasphere associated with substorm-injected electrons, *Geophys. Res. Lett.*, **40**, 3798–3803, doi:10.1002/grl.50787.
- Li, X., I. Roth, M. Temerin, J. R. Wygant, M. K. Hudson, and J. B. Blake (1993), Simulation of the prompt energization and transport of radiation belt particles during the March 24, 1991 SSC, *Geophys. Res. Lett.*, **20**, 2423–2426, doi:10.1029/93GL02701.
- Lyons, L. R., and R. M. Thorne (1973), Equilibrium structure of radiation belt electrons, *J. Geophys. Res.*, **78**, 2142–2149, doi:10.1029/JA078i013p02142.
- Mauk, B. H., N. J. Fox, S. G. Kanekal, R. L. Kessel, D. G. Sibeck, and A. Ukhorskiy (2013), Science objectives and rationale for the radiation belt storm probes mission, *Space Sci. Rev.*, **179**, 3–27, doi:10.1007/s11214-012-9908-y.
- McComas, D. J., S. J. Bame, P. Barker, W. C. Feldman, J. L. Phillips, P. Riley, and J. W. Griffee (1998), Solar Wind Electron Proton Alpha Monitor (SWEPAM) for the advanced composition explorer, *Space Sci. Rev.*, **86**, 563–612, doi:10.1023/A:1005040232597.
- Meredith, N. P., R. B. Horne, R. M. Thorne, D. Summers, and R. R. Anderson (2004), Substorm dependence of plasmaspheric hiss, *J. Geophys. Res.*, **109**, A06209, doi:10.1029/2004JA010387.
- Meredith, N. P., R. B. Horne, S. A. Glauert, and R. R. Anderson (2007), Slot region electron loss timescales due to plasmaspheric hiss and lightning-generated whistlers, *J. Geophys. Res.*, **112**, A08214, doi:10.1029/2007JA012413.
- Meurant, M., J. Gérard, C. Blockx, B. Hubert, and V. Coumans (2004), Propagation of electron and proton shock-induced aurora and the role of the interplanetary magnetic field and solar wind, *J. Geophys. Res.*, **109**, A10210, doi:10.1029/2004JA010453.
- Mourenas, D., and J.-F. Ripoll (2012), Analytical estimates of quasi-linear diffusion coefficients and electron lifetimes in the inner radiation belt, *J. Geophys. Res.*, **117**, A01204, doi:10.1029/2011JA016985.
- Ni, B., et al. (2014), Resonant scattering of energetic electrons by unusual low-frequency hiss, *Geophys. Res. Lett.*, **41**, 1854–1861, doi:10.1002/2014GL059389.
- Nunn, D., Y. Omura, H. Matsumoto, I. Nagano, and S. Yagitani (1997), The numerical simulation of VLF chorus and discrete emissions observed on the Geotail satellite using a Vlasov code, *J. Geophys. Res.*, **102**, 27,083–27,098, doi:10.1029/97JA02518.
- Omura, Y., Y. Katoh, and D. Summers (2008), Theory and simulation of the generation of whistler-mode chorus, *J. Geophys. Res.*, **113**, A04223, doi:10.1029/2007JA012622.
- Peng, Z., C. Wang, Y. Q. Hu, J. R. Kan, and Y. F. Yang (2011), Simulations of observed auroral brightening caused by solar wind dynamic pressure enhancements under different interplanetary magnetic field conditions, *J. Geophys. Res.*, **116**, A06217, doi:10.1029/2010JA016318.
- Reeves, G. D., D. N. Baker, R. D. Belian, J. B. Blake, T. E. Cayton, J. F. Fennell, R. H. W. Friedel, M. M. Meier, R. S. Selesnick, and H. E. Spence (1998), The global response of relativistic radiation belt electrons to the January 1997 magnetic cloud, *Geophys. Res. Lett.*, **25**, 3265–3268, doi:10.1029/98GL02509.
- Ronnmark, K. (1982), Waves in homogeneous, anisotropic, multicomponent plasmas, *Kiruna Rep. No. 179*. Kiruna Geophys. Inst., Kiruna, Sweden, 55 pp.
- Russell, C. T., R. E. Holzer, and E. J. Smith (1969), OGO 3 observations of ELF noise in the magnetosphere: 1. Spatial extent and frequency of occurrence, *J. Geophys. Res.*, **74**, 755–777, doi:10.1029/JA074i003p00755.
- Samsonov, A. A., D. G. Sibeck, and J. Imber (2007), MHD simulation for the interaction of an interplanetary shock with the Earth's magnetosphere, *J. Geophys. Res.*, **112**, A12220, doi:10.1029/2007JA012627.
- Sheeley, R. W., M. B. Moldwin, H. K. Rassoul, and R. R. Anderson (2001), An empirical plasmasphere and trough density model: CRRES observations, *J. Geophys. Res.*, **106**, 25,631–25,642, doi:10.1029/2000JA000286.
- Shklyar, D. R. (2011), Wave-particle interactions in marginally unstable plasma as a means of energy transfer between energetic particle populations, *Phys. Lett. A*, **375**, 1583–1587, doi:10.1016/j.physleta.2011.02.067.
- Shprits, Y. Y., D. Subbotin, and B. Ni (2009), Evolution of electron fluxes in the outer radiation belt computed with the VERB code, *J. Geophys. Res.*, **114**, A11209, doi:10.1029/2008JA013784.
- Shue, J., et al. (1998), Magnetopause location under extreme solar wind conditions, *J. Geophys. Res.*, **103**, 17,691–17,700, doi:10.1029/98JA01103.
- Smith, C. W., J. L'Heureux, N. F. Ness, M. H. Acuña, L. F. Burlaga, and J. Scheifele (1998), The ACE magnetic fields experiment, *Space Sci. Rev.*, **86**, 613–632, doi:10.1023/A:1005092216668.
- Sonwalkar, V. S., and U. S. Inan (1989), Lightning as an embryonic source of VLF hiss, *J. Geophys. Res.*, **94**, 6986–6994, doi:10.1029/JA094iA06p06986.
- Spence, H. E., et al. (2013), Science goals and overview of the energetic particle, composition, and thermal plasma (ECT) suite on NASA's Radiation Belt Storm Probes (RBSP) mission, *Space Sci. Rev.*, **179**, 311–336, doi:10.1007/s11214-013-0007-5.
- Stone, E. C., A. M. Frandsen, R. A. Mewaldt, E. R. Christian, D. Margolies, J. F. Ormes, and F. Snow (1998), The advanced composition explorer, *Space Sci. Rev.*, **86**, 1–22, doi:10.1023/A:1005082526237.
- Su, Z., F. Xiao, H. Zheng, and S. Wang (2010), STEERB: A three-dimensional code for storm-time evolution of electron radiation belt, *J. Geophys. Res.*, **115**, A09208, doi:10.1029/2009JA015210.
- Su, Z., F. Xiao, H. Zheng, and S. Wang (2011a), CRRES observation and STEERB simulation of the 9 October 1990 electron radiation belt dropout event, *Geophys. Res. Lett.*, **38**, L06106, doi:10.1029/2011GL046873.
- Su, Z., F. Xiao, H. Zheng, and S. Wang (2011b), Radiation belt electron dynamics driven by adiabatic transport, radial diffusion, and wave-particle interactions, *J. Geophys. Res.*, **116**, A04205, doi:10.1029/2010JA016228.
- Su, Z., Q. Zong, C. Yue, Y. Wang, H. Zhang, and H. Zheng (2011c), Proton auroral intensification induced by interplanetary shock on 7 November 2004, *J. Geophys. Res.*, **116**, A08223, doi:10.1029/2010JA016239.
- Su, Z., et al. (2014), Intense duskside lower band chorus waves observed by Van Allen Probes: Generation and potential acceleration effect on radiation belt electrons, *J. Geophys. Res. Space Physics*, **119**, 4266–4273, doi:10.1002/2014JA019919.

- Subbotin, D., Y. Shprits, and B. Ni (2010), Three-dimensional VERB radiation belt simulations including mixed diffusion, *J. Geophys. Res.*, **115**, A03205, doi:10.1029/2009JA015070.
- Summers, D., R. M. Thorne, and F. Xiao (1998), Relativistic theory of wave-particle resonant diffusion with application to electron acceleration in the magnetosphere, *J. Geophys. Res.*, **103**, 20,487–20,500.
- Summers, D., B. Ni, N. P. Meredith, R. B. Horne, R. M. Thorne, M. B. Moldwin, and R. R. Anderson (2008), Electron scattering by whistler-mode elf hiss in plasmaspheric plumes, *J. Geophys. Res.*, **113**, A04219, doi:10.1029/2007JA012678.
- Summers, D., Y. Omura, S. Nakamura, and C. A. Kletzing (2014), Fine structure of plasmaspheric hiss, *J. Geophys. Res. Space Physics*, **119**, 9134–9149, doi:10.1002/2014JA020437.
- Thorne, R. M., E. J. Smith, R. K. Burton, and R. E. Holzer (1973), Plasmaspheric hiss, *J. Geophys. Res.*, **78**, 1581–1596, doi:10.1029/JA078i010p01581.
- Thorne, R. M., E. J. Smith, K. J. Fiske, and S. R. Church (1974), Intensity variation of ELF hiss and chorus during isolated substorms, *Geophys. Res. Lett.*, **1**, 193–196, doi:10.1029/GL001i005p00193.
- Thorne, R. M., S. R. Church, and D. J. Gorney (1979), On the origin of plasmaspheric hiss—The importance of wave propagation and the plasmapause, *J. Geophys. Res.*, **84**, 5241–5247, doi:10.1029/JA084iA09p05241.
- Thorne, R. M., et al. (2013), Evolution and slow decay of an unusual narrow ring of relativistic electrons near $L \sim 3.2$ following the September 2012 magnetic storm, *Geophys. Res. Lett.*, **40**, 3507–3511, doi:10.1002/grl.50627.
- Tsurutani, B. T., et al. (2001), Auroral zone dayside precipitation during magnetic storm initial phases, *J. Atmos. Sol. Terr. Phys.*, **63**, 513–522, doi:10.1016/S1364-6826(00)00161-9.
- Tsurutani, B. T., B. J. Falkowski, J. S. Pickett, O. Santolik, and G. S. Lakhina (2015), Plasmaspheric hiss properties: Observations from polar, *J. Geophys. Res. Space Physics*, **120**, 414–431, doi:10.1002/2014JA020518.
- Tu, W., G. S. Cunningham, Y. Chen, M. G. Henderson, E. Camporeale, and G. D. Reeves (2013), Modeling radiation belt electron dynamics during GEM challenge intervals with the DREAM3D diffusion model, *J. Geophys. Res. Space Physics*, **118**, 6197–6211, doi:10.1002/jgra.50560.
- Turner, D. L., Y. Shprits, M. Hartinger, and V. Angelopoulos (2012), Explaining sudden losses of outer radiation belt electrons during geomagnetic storms, *Nat. Phys.*, **8**, 208–212, doi:10.1038/nphys2185.
- Ukhorskiy, A. Y., and M. I. Sitnov (2013), Dynamics of radiation belt particles, *Space Sci. Rev.*, **179**, 545–578, doi:10.1007/s11214-012-9938-5.
- Wang, C., T. R. Sun, X. C. Guo, and J. D. Richardson (2010), Case study of nightside magnetospheric magnetic field response to interplanetary shocks, *J. Geophys. Res.*, **115**, A10247, doi:10.1029/2010JA015451.
- Wygant, J., et al. (2013), The electric field and waves instruments on the radiation belt storm probes mission, *Space Sci. Rev.*, **179**(1–4), 183–220, doi:10.1007/s11214-013-0013-7.
- Zhang, H., D. G. Sibeck, Q.-G. Zong, J. P. McFadden, D. Larson, K.-H. Glassmeier, and V. Angelopoulos (2012), Global magnetospheric response to an interplanetary shock: THEMIS observations, *Ann. Geophys.*, **30**, 379–387, doi:10.5194/angeo-30-379-2012.
- Zhou, X., and B. T. Tsurutani (1999), Rapid intensification and propagation of the dayside aurora: Large scale interplanetary pressure pulses (fast shocks), *Geophys. Res. Lett.*, **26**, 1097–1100.
- Zong, Q., X. -Z. Zhou, Y. F. Wang, X. Li, P. Song, D. N. Baker, T. A. Fritz, P. W. Daly, M. Dunlop, and A. Pedersen (2009), Energetic electron response to ULF waves induced by interplanetary shocks in the outer radiation belt, *J. Geophys. Res.*, **114**, A10204, doi:10.1029/2009JA014393.